

A three-dimensional NMR experiment with improved sensitivity for carbonyl–carbonyl J correlation in proteins

Stephan Grzesiek and Ad Bax

Laboratory of Chemical Physics, National Institutes of Diabetes and Digestive and Kidney Diseases, National Institutes of Health, Bethesda, MD 20892-0520, U.S.A.

Received 2 January 1997

Accepted 5 February 1997

Keywords: Carbon–carbon J coupling; HOHAHA; TOCSY; Relaxation; ϕ Angle; HIV-1 Nef; Ubiquitin

Summary

Recently, a quantitative J correlation technique has been presented that permits measurement of ${}^3J_{C'_{i-1}C'_i}$ in proteins isotopically enriched with ${}^{13}\text{C}$ [Hu, J.-S. and Bax, A. (1996) *J. Am. Chem. Soc.*, **118**, 8170–8171]. Here, we describe an analogous experiment that is less sensitive to transverse ${}^{13}\text{C}$ relaxation, which is the principal limiting factor in all ${}^{13}\text{C}$ – ${}^{13}\text{C}$ long-range correlation experiments on macromolecules. The new scheme utilizes homonuclear Hartmann–Hahn cross polarization (TOCSY) instead of a COSY-type transfer to accomplish magnetization transfer; a description of the relevant relaxation terms is presented. The experiment is demonstrated for ubiquitin and HIV-1 Nef. The results show excellent agreement between ${}^3J_{C'_{i-1}C'_i}$ values measured for ubiquitin with the new scheme and those reported previously. The experiment is particularly useful for distinguishing backbone ϕ angles that are smaller than -120° from those larger than -120° .

For most amino acid residue types, six different J couplings are available to characterize the backbone angle ϕ : ${}^3J_{\text{H}^{\text{N}}\text{H}^\alpha}$, ${}^3J_{\text{H}^{\text{N}}\text{C}^\beta}$, ${}^3J_{\text{H}^{\text{N}}\text{C}'}$, ${}^3J_{\text{C}'\text{H}^\alpha}$, ${}^3J_{\text{C}'\text{C}^\beta}$, and ${}^3J_{\text{C}'\text{C}'}$. Of this set, ${}^3J_{\text{H}^{\text{N}}\text{H}^\alpha}$ is clearly the coupling that is easiest to measure and it has become widely used in protein structure determination (Pardi et al., 1984; Wüthrich, 1986; Garrett et al., 1994). However, due to the symmetry of the Karplus relation about $\phi = -120^\circ$, this coupling alone does not allow one to distinguish $\phi = -120^\circ + \alpha$ from $\phi = -120^\circ - \alpha$. Considering the shapes of the Karplus curves for the other five couplings (Hu and Bax, 1996; Wang and Bax, 1996; J.-S. Hu and A. Bax, manuscript submitted), ${}^3J_{\text{C}'\text{C}'}$ is best suited for lifting this degeneracy, as it has its steepest ϕ dependence near $\phi = -120^\circ$. Its value is described by the Karplus equation ${}^3J_{\text{C}'\text{C}'} = 1.33 \cos^2\phi - 0.88 \cos\phi + 0.62$ Hz, and the root-mean-square difference between the measured values and those predicted by this equation, using crystal structure ϕ angles, was only 0.16 Hz (Hu and Bax, 1996). These ${}^3J_{\text{C}'\text{C}'}$ values were measured using a quantitative J correlation technique named HN(CO)CO, in which magnetization was transferred in an 'out-and-back' manner from a backbone carbonyl to its adjacent ones. The small magnitude of ${}^3J_{\text{C}'\text{C}'}$ mandates the use of relatively long C' dephasing and rephasing intervals in this experiment and

application of this technique was restricted to proteins with short rotational correlation times. Here, we demonstrate that a significant increase in signal-to-noise can be obtained if magnetization is transferred with an isotropic mixing scheme instead of the regular 'COSY-type' scheme, thereby extending the measurement of ${}^3J_{\text{C}'\text{C}'}$ to proteins with less favorable relaxation properties.

It has long been recognized that magnetization transfer during isotropic mixing occurs faster than in pulse-interrupted free precession methods and therefore offers the possibility to increase sensitivity (Braunschweiler and Ernst, 1983; Bax and Davis, 1985; Schleucher et al., 1995). However, in order to assess quantitatively whether a net gain in sensitivity can be obtained by the use of isotropic mixing, the relevant relaxation terms must be considered as well. We present a simple analysis of these terms and demonstrate that the use of isotropic mixing can indeed result in a significant improvement in sensitivity, making ${}^{13}\text{C}'$ – ${}^{13}\text{C}'$ correlation also feasible for proteins with rotational correlation times in excess of 10 ns.

In the new scheme (Fig. 1), magnetization is transferred from an amide proton, ${}^1\text{H}_i^{\text{N}}$, via its attached ${}^{15}\text{N}_i$ (time point a), to ${}^{13}\text{C}'_{i-1}$ (time b). After ${}^{13}\text{C}'_{i-1}$ magnetization has refocused during the constant-time ${}^{13}\text{C}'$ evolution period

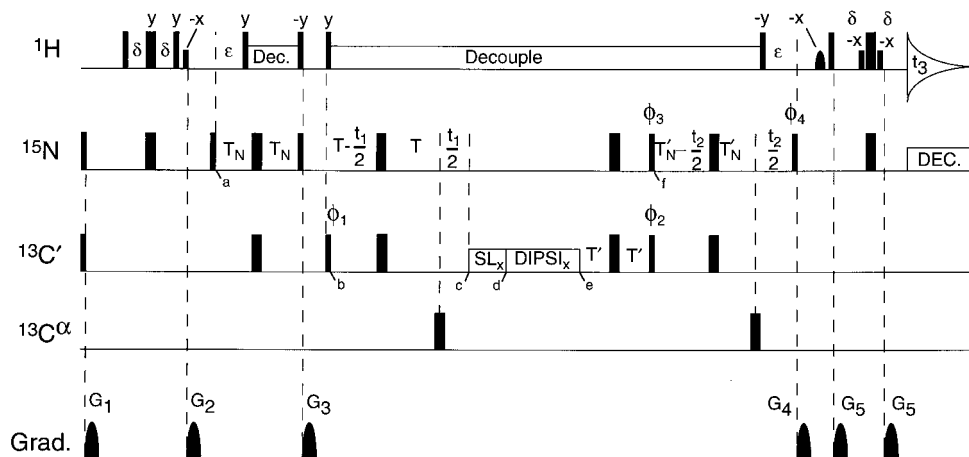


Fig. 1. Pulse sequence of the 3D (HN)CO(CO)NH experiment. Narrow and wide denote 90° and 180° flip angles, respectively, and unless indicated the phase is x . SL_x denotes a 2-ms spin-lock pulse ($\gamma_C B_2 = 5$ kHz), applied along the x -axis. DIPSI $_x$ refers to the application of isotropic mixing, using the DIPSI-3 (Shaka et al., 1988) mixing scheme, with the rf field ($\gamma_C B_2 = 2.8$ kHz) applied along the $\pm x$ -axis. 1H decoupling is applied using a DIPSI-2 modulation scheme ($\gamma_H B_1 = 5$ kHz; phase x), with the carrier at the H_2O resonance. Rectangular low-power 1H pulses are applied using $\gamma_H B_1 = 200$ Hz. The shaped 90° pulse has a sine-bell amplitude profile and a duration of 2.3 ms. All $^{13}C'$ and $^{13}C^\alpha$ pulses are applied at an rf field strength $\gamma_C B_2 = \sqrt{15} \Delta\delta$, where $\Delta\delta$ is the difference in resonance frequency between the ^{13}C carrier and the center of the carbonyl region, such that the excitation profile of a rectangular 90° $^{13}C'$ pulse has a null at $^{13}C^\alpha$, and vice versa. Delay durations: $\delta = 2.3$ ms; $\varepsilon = 5.3$ ms; $T_N = 13.5$ ms; $T = 13.5$ ms; $T' = 13.5$ ms; $T_N = 13.5$ ms. Phase cycling: $\phi_1 = x$; $\phi_2 = 4(x), 4(-x)$; $\phi_3 = x, -x$; $\phi_4 = 2(x), 2(-x)$; receiver = $x, 2(-x), x, -x, 2(x), -x$. Quadrature detection in the t_1 and t_2 dimensions is obtained by altering ϕ_1 and ϕ_3 in the States-TPPI manner, respectively. Gradients (sine-bell shaped; 25 G/cm at the center): $G_{1,2,3,4,5} = 1, 1, 2.1, 1.7, \text{ and } 0.4$ ms.

to become in-phase with respect to $^{15}N_i$ (point c), it is subjected to a short spin-lock pulse, in order to dephase net magnetization orthogonal to the spin-lock field, followed by isotropic mixing with a DIPSI-3 (Shaka et al., 1988) pulse scheme (time points d to e), during which part of its magnetization is transferred to $^{13}C'_{i-2}$ and $^{13}C'_i$. Subsequently, $^{13}C'$ magnetization is dephased with respect to its adjacent ^{15}N , transferred to ^{15}N (time f) and, after a ^{15}N constant-time evolution period, transferred to H^N for detection during t_3 . A fraction (which depends on $^3J_{C'C_i}$) of the magnetization flows sequentially from $^1H_i^N$ to its $^{15}N_i$, to $^{13}C'_{i-1}$, to $^{13}C'_i$ (and to $^{13}C'_{i-2}$), to $^{15}N_{i+1}$ ($^{15}N_{i-1}$), to $^1H_{i+1}^N$ ($^1H_{i-1}^N$), with evolution on $^{13}C'_{i-1}$ and $^{15}N_{i+1}$, and detection of $^1H_{i+1}^N$, and we therefore name the experiment (HN)CO(CO)NH. $^{13}C'$ magnetization that is not transferred to its $^{13}C'$ neighbors during the isotropic mixing period gives rise to a 'diagonal' resonance with the $^{13}C'_{i-1}$ frequency in F1, $^{15}N_i$ in F2 and $^1H_i^N$ in F3. The pulse scheme shown in Fig. 1 includes water flip-back pulses (Grzesiek and Bax, 1993; Kay et al., 1994) in order to minimize saturation of the H_2O signal.

The magnetization transfer process is very similar to that of all other triple resonance experiments and can be described in terms of the product operator formalism. In order to evaluate the efficiency of the (HN)CO(CO)NH experiment relative to that of the HN(CO)CO scheme, we will first provide the pertinent product operator terms for the interval between time points b and f, where the new experiment differs from the original one. Subsequently, we will analyze the effects of $^{13}C'$ relaxation. For reasons of simplicity, the effects of ^{15}N and $^{13}C^\alpha$ longitudinal

relaxation are ignored and we consider a system of only two carbonyl spins, I and S. Evolution resulting from $^{13}C'$ chemical shifts between time points b and c is refocused (for the first t_1 increment) and the same applies between e and f. Chemical shifts are therefore ignored in the description given below.

At time point b, $^{13}C'$ magnetization of spin I is described by I_x (it actually is $-2I_y N_z$, but the $-2I_y N_z$ refocuses to I_x during the $2T$ interval). As a result of J coupling to the second $^{13}C'$, S, it evolves to yield a density matrix, σ_c , given by:

$$\sigma_c = I_x \cos\phi_1 + 2 I_y S_z \sin\phi_1 \quad (1)$$

with $\phi_1 = 2\pi J_{C'C_i} T$. $^{13}C^\alpha$ is decoupled from $^{13}C'$ by the application of a selective 180° $^{13}C^\alpha$ pulse and no net $J_{C'C^\alpha}$ dephasing has occurred at time point c. The subsequent 1-ms spin-lock period can be considered as a θ_x pulse, resulting in:

$$\sigma_d = I_x \cos\phi_1 + 2 I_y S_z \sin\phi_1 \cos^2\theta - 2 I_y S_y \sin\phi_1 \sin^2\theta - I_y S_y \sin\phi_1 \sin(2\theta) + I_z S_z \sin\phi_1 \sin(2\theta) \quad (2)$$

As a result of inhomogeneity of the radiofrequency field, the angle θ is distributed uniformly between 0 and 2π over the sample volume and the last two terms in Eq. 2 average to zero. The values of $\sin^2(\theta)$ and $\cos^2(\theta)$, averaged over the sample volume, are 1/2. Thus, Eq. 2 may be rewritten as:

$$\sigma_d = I_x \cos\phi_1 + (I_y S_z - I_z S_y) \sin\phi_1 \quad (3)$$

To describe the evolution during isotropic mixing, the following short notations are used (Ernst et al., 1987):

$$\Sigma_{\alpha} = I_{\alpha} + S_{\alpha} \quad (4a)$$

$$\Sigma_{\alpha\beta} = 2(I_{\alpha}S_{\beta} + I_{\beta}S_{\alpha}) \quad (4b)$$

$$\Delta_{\alpha} = I_{\alpha} - S_{\alpha} \quad (4c)$$

$$\Delta_{\alpha\beta} = 2(I_{\alpha}S_{\beta} - I_{\beta}S_{\alpha}) \quad (4d)$$

where (α, β, γ) are cyclic permutations of (x, y, z) . Applicable commutation relations are:

$$[I \cdot S, \Sigma_{\alpha}] = 0 \quad (4e)$$

$$[I \cdot S, \Sigma_{\alpha\beta}] = 0 \quad (4f)$$

$$[I \cdot S, \Delta_{\alpha}] = i \Delta_{\beta\gamma} \quad (4g)$$

$$[I \cdot S, \Delta_{\alpha\beta}] = -i \Delta_{\gamma} \quad (4h)$$

In the notation of Eq. 4, Eq. 3 transforms into:

$$\sigma_d = \frac{1}{2} \Sigma_x \cos \phi_1 + \frac{1}{2} \Delta_x \cos \phi_1 + \frac{1}{2} \Delta_{yz} \sin \phi_1 \quad (5)$$

Evolution under influence of the scalar coupling Hamiltonian $J_{C'C} I \cdot S$ for a duration τ_m yields a density matrix at time point e, given by:

$$\sigma_e = \frac{1}{2} \Sigma_x \cos \phi_1 + \frac{1}{2} \Delta_x \cos(\phi_1 + \phi_2) + \frac{1}{2} \Delta_{yz} \sin(\phi_1 + \phi_2) \quad (6)$$

where $\phi_2 = 2\pi J_{C'C} \tau_m$. Evolution during the following $J_{C'N}$ dephasing interval of duration $2T'$ ($2T' \approx (2J_{C'N})^{-1}$), and using $\phi_3 = 2\pi J_{C'C} T'$, yields a density matrix at time f given by:

$$\begin{aligned} \sigma_f = & \frac{1}{2} \Sigma_x \cos \phi_1 \cos \phi_3 + \frac{1}{2} \Sigma_{yz} \cos \phi_1 \sin \phi_3 \\ & + \frac{1}{2} \Delta_x \cos(\phi_1 + \phi_2 + \phi_3) + \frac{1}{2} \Delta_{yz} \sin(\phi_1 + \phi_2 + \phi_3) \end{aligned} \quad (7a)$$

where, for brevity, the effect of $J_{C'N}$ dephasing again has not been included. Only in-phase I_x and S_x components of σ_f are converted back to observable H^N magnetization, and these terms are given by:

$$\begin{aligned} \sigma_{f, \text{in-phase}} = & \frac{1}{2} [\cos \phi_1 \cos \phi_3 + \cos(\phi_1 + \phi_2 + \phi_3)] I_x \\ & + \frac{1}{2} [\cos \phi_1 \cos \phi_3 - \cos(\phi_1 + \phi_2 + \phi_3)] S_x \end{aligned} \quad (7b)$$

Here the I_x and S_x coefficients refer to the diagonal and cross-peak peak intensities, respectively, and the cross-peak to diagonal-peak intensity ratio equals:

$$I_C/I_D = \frac{[\cos \phi_1 \cos \phi_3 - \cos(\phi_1 + \phi_2 + \phi_3)]}{[\cos \phi_1 \cos \phi_3 + \cos(\phi_1 + \phi_2 + \phi_3)]} \quad (8)$$

Next, we will analyze the effects of relaxation during the isotropic mixing period, with the radiofrequency field applied along the $\pm x$ -axis and the in-phase magnetization residing along x . Σ_x and Δ_x remain aligned along the x -

axis during the mixing scheme, and relax at the $^{13}C'$ transverse relaxation rate, R_2 . Assuming that the individual terms in the operator products relax independently, i.e., ignoring cross correlation, the $I_y S_z$ and $I_z S_y$ terms relax during x -axis rf irradiation at the sum of the relaxation rates applicable for the individual I_y , S_y , I_z and S_z terms. Magnetization orthogonal to the rf field, in the yz plane, spends on average half its time along the z -axis and relaxes at a rate $(R_1 + R_2)/2$, where R_1 is the longitudinal relaxation rate (Abragam, 1961). Therefore, $I_y S_z$ and $I_z S_y$ terms relax at an antiphase relaxation rate, $R_{a.p.} = R_1 + R_2$. As in proteins $R_2 \gg R_1$, to a good approximation relaxation during the isotropic mixing scheme attenuates all terms in Eq. 7 by the same factor, $\exp(-R_2 \tau_m)$.

Maximum intensity of the cross peak (i.e., maximum sensitivity of the experiment) is obtained when the derivative of $[\cos \phi_1 \cos \phi_3 - \cos(\phi_1 + \phi_2 + \phi_3)] \exp(-R_2 \tau_m)$ with respect to the duration of the mixing period, τ_m , is zero. For $J_{C'C} \ll R_2$ and $(R_2 T)^2 \ll 1$, this occurs when $\tau_m \approx 2/R_2 - T - T'$, yielding a cross-peak intensity $I_C \approx 4(\pi J_{C'C}/R_2)^2 \exp[-2 - R_2(T + T')]$. For $J_{C'C} \ll R_2$, the original experiment (Hu and Bax, 1996) is optimized for sensitivity when $^{13}C'$ de- and rephasing intervals of duration $\tau = 1/R_2$ are used, yielding a cross-peak intensity $I_C \approx (\pi J_{C'C}/R_2)^2 \exp(-2)$. Thus, for the two-spin case in the $J_{C'C} \ll R_2$ limit, the (HN)CO(CO)NH experiment yields an increase in sensitivity by a factor $4 \times \exp[-R_2(T + T')]$ over the original experiment. To ensure the validity of the two-spin approximation, it is recommended that τ_m in the (HN)CO(CO)NH experiment is set no longer than ~ 125 ms. Therefore, for proteins with $R_2 \leq \sim 12$ s^{-1} , the gain in sensitivity obtained with the (HN)CO(CO)NH experiment is somewhat smaller than calculated above.

To a first approximation, the value of $J_{C'C}$ can be extracted from the I_C/I_D ratio, using Eq. 8. This equation, however, does not account for the fact that different spins in the protein in general will have different relaxation rates. The cumulative loss resulting from relaxation and imperfect pulses during magnetization transfer from amide proton n to its adjacent carbonyl, between the start of the pulse scheme and time point b in Fig. 1, equals a factor $A(n)$. Similarly, a loss factor $B(n)$ applies between time point f and data acquisition. If the transfer of magnetization from spin n to spin m , occurring between time points b and f, is described by a factor $T(n, m)$, the corresponding resonance intensities, $I(n, m)$, of the diagonal ($m = n$) and cross peaks ($m = n \pm 1$) are given by $I(n, m) = A(n) T(n, m) B(m)$. For reasons of symmetry, $T(n, m) = T(m, n)$ (Griesinger et al., 1987). Equation 8 ignores the loss factors and assumes $I_C/I_D = T(n, m)/T(n, n)$, i.e., it assumes that $B(n) = B(m)$, which is generally not true. However, if the intensities of both the (n, n) and (m, m) diagonal peaks and the (n, m) and (m, n) cross peaks can be measured, the value of $J_{C'C}$ can be derived from these data in a manner independent of the factors $A(n)$ and $B(n)$:

$$\frac{[I(n,m) \times I(m,n)] / [I(n,n) \times I(m,m)]}{[T(n,m) \times T(m,n)] / [T(n,n) \times T(m,m)]} = \quad (9)$$

Thus, $\{[I(n,m) \times I(m,n)] / [I(n,n) \times I(m,m)]\}^{1/2}$ corresponds to the I_C/I_D ratio of Eq. 8, and permits calculation of $J_{C'C}$ in a manner independent of variations in $A(n)$ and $B(n)$. If the set of cross peaks and diagonal peaks for two coupled $^{13}C'$ spins is incomplete, an approximate value for $J_{C'C}$ can be obtained by assuming that $A(n) = A(m)$ and $B(n) = B(m)$.

Experiments were carried out for samples containing 3.5 mg $^{13}C/^{15}N$ -enriched ubiquitin (pH 4.7; 30 °C) in a 220 μ l Shigemi microcell (1.8 mM), and 16 mg HIV-1 Nef^{62-39, Δ 159-173} in 1.6 ml (0.6 mM), 95% $H_2O/5\%$ D_2O , pH 8.0, 35 °C. Both spectra were recorded on a Bruker DMX-600 spectrometer as $54^* \times 24^* \times 512^*$ data sets, with acquisition times of 27, 27, and 56 ms in the t_1 , t_2 , and t_3 dimension, respectively. The total recording times were 13.8 h for ubiquitin and 68 h for Nef. The durations of the isotropic mixing period were 117 ms for ubiquitin and 98 ms for Nef.

Figure 2 shows $^{13}C'$ strips taken from the 3D spectra of both proteins for a set of sequential amide residues. As shown in Fig. 3, $^3J_{C'C}$ values derived from the ubiquitin spectrum generally are in excellent agreement with previously published values. Significant deviations between the observed and predicted intensity ratios are only observed for Ile⁴⁴ and Phe⁴⁵, which yield ratios (using Eq. 9) corresponding to $J_{C'C}$ values that are 0.25 Hz (Leu⁴³ C'-Ile⁴⁴ C') and 0.16 Hz (Ile⁴⁴ C'-Phe⁴⁵ C') larger than predicted on

the basis of the previously published $J_{C'C}$ values. This discrepancy is caused by the two-spin approximation in the calculations presented above. As Ile⁴⁴ C' has relatively large $J_{C'C}$ couplings to both Leu⁴³ C' and Phe⁴⁵ C', its diagonal resonance is attenuated more than predicted by Eq. 7b. A quantitative interpretation using Eqs. 8 and 9 is valid only if the two-spin approximation applies, i.e., where there is no third $^{13}C'$, B, for which the relation $2\pi J_{C'B}\tau_m \ll 1$ is not valid. From a practical perspective, both computer simulations and the ubiquitin spectra indicate that quantitative interpretation of the cross-peak to diagonal-peak intensity ratio, using Eq. 9, yields a significant error only when two cross peaks are observed for a given amide that are both considerably more intense than the diagonal resonance. For example, the diagonal for Ile⁴⁴ C' is threefold weaker than its cross peaks to Leu⁴³ C' and Phe⁴⁵ C', resulting in the above-mentioned discrepancy. For the Val¹⁷ strip in Fig. 2A, where its cross peak to Val¹⁷ C' is also nearly three times stronger than its Glu¹⁶ C' diagonal, but its cross peak to Leu¹⁵ C' is fourfold weaker, no significant error is introduced.

Clearly, owing to its short rotational correlation time ($\tau_c \approx 4.1$ ns) and high sample concentration, ubiquitin yields a considerably higher signal-to-noise ratio than the HIV-1 Nef ($\tau_c \approx 12$ ns) spectrum. Nevertheless, as can be seen in Fig. 2B, the signal-to-noise ratio of the Nef spectrum is sufficiently high to allow identification of sequential $^{13}C'$ - $^{13}C'$ connectivities in β -sheet regions of the protein. Residues Arg¹⁷⁸-Val¹⁸⁰ have backbone mobilities above average and show intense diagonal resonances (Fig.

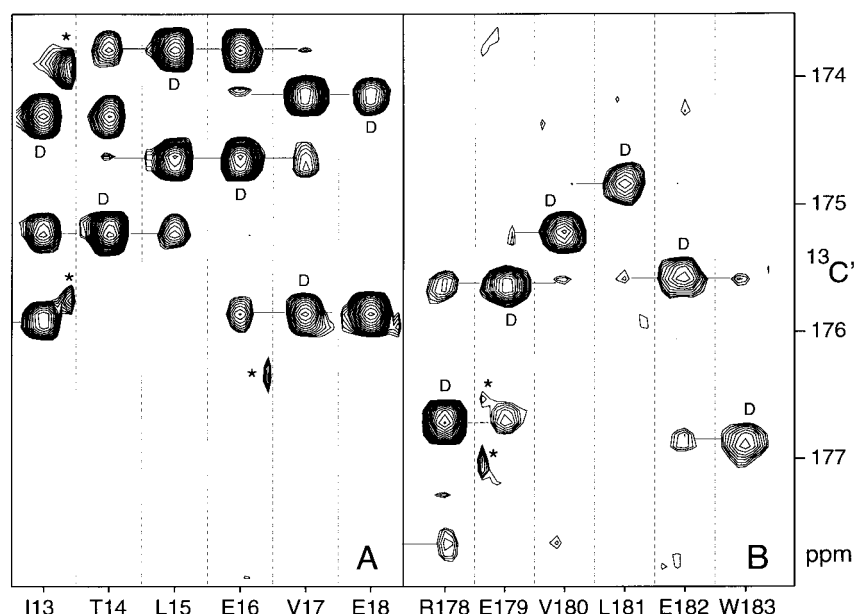


Fig. 2. F1 strips from the 3D (HN)CO(CO)NH spectra of (A) 1.8 mM ubiquitin, taken at the $^1H^N$ (F3) and ^{15}N (F2) frequencies of Ile¹³-Glu¹⁸, and (B) 0.6 mM Nef, taken at the $^1H^N/^{15}N$ frequencies of Arg¹⁷⁸-Trp¹⁸³. Correlations from residues with $^1H^N$ and ^{15}N shifts in the vicinity of the selected amide strip are marked '*'; diagonal peaks, corresponding to the $^{13}C'$ of the residue preceding the amide, are marked 'D'. The low signal-to-noise ratio of the Nef spectrum relative to the ubiquitin spectrum results primarily from the about threefold longer effective rotational correlation time of Nef, yielding $^{13}C'$ T_2 values (at 151 MHz) of ~ 50 ms for Nef, and ~ 130 ms for ubiquitin. As a result of the long mixing time (117 ms), the ubiquitin spectrum shows weak relay correlations between Ile¹³ C' and Leu¹⁵ C', Thr¹⁴ C' and Glu¹⁶ C', and Leu¹⁵ C' and Val¹⁷ C'.

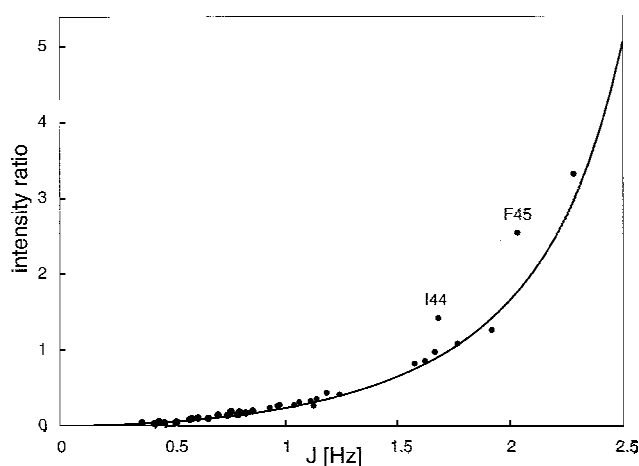


Fig. 3. Relation between the previously reported ubiquitin $J_{C'}$ values and the cross-peak to diagonal-peak intensity ratio derived from the square root of Eq. 9. The drawn line is the intensity ratio predicted using Eq. 8, for a 117-ms isotropic mixing period duration, and T and T' durations of 13.5 ms. Intensity ratios observed for Ile⁴⁴ and Phe⁴⁵ are larger than predicted because the Ile⁴⁴ $^{13}C'$ resonance has large couplings to both Leu⁴³ C' (1.7 Hz) and Phe⁴⁵ C' (2.0 Hz), making the two-spin approximation, used for deriving Eq. 8, invalid for the long mixing time used (see text).

2B). Leu¹⁸¹-Trp¹⁸³, on the other hand, are located near the center of the fifth β -strand and ^{15}N relaxation studies indicate no increased mobility for these residues (S. Grzesiek et al., manuscript submitted). Cross-peak to diagonal-peak intensity ratios for Arg¹⁷⁸-Trp¹⁸³ correspond to $^3J_{C'C'}$ couplings in the 1–1.5 Hz range, which translates into ϕ angles in the -125 to -105° range. For most residues outside of the Nef β -sheet, no sequential $^{13}C'$ - $^{13}C'$ connectivities are observed. The absence of a $^{13}C'$ - $^{13}C'$ cross peak can be interpreted in terms of an upper limit of the cross-peak to diagonal-peak ratio, which translates into an upper limit for $^3J_{C'C'}$. In the absence of $^3J_{C'C'}$ -derived ϕ angle restraints, the relatively low number of NOE cross peaks obtained for HIV-1 Nef resulted in structures with a substantial fraction of residues having unfavorable ϕ angles, smaller than -145° (Grzesiek et al., 1996). With inclusion of the $^3J_{C'C'}$ -derived ϕ restraints, the fraction of residues with backbone angles in the most favorable region of the Ramachandran map, as defined by the program PROCHECK-NMR (Laskowski et al., 1996) increases from 64 to 73%.

In summary, we have shown that the (HN)CO(CO)NH experiment considerably improves the sensitivity of $^3J_{C'C'}$ measurements relative to the HN(CO)CO experiment, thereby extending the applicability of this type of measurement to larger proteins. The increase in sensitivity results from the use of homonuclear isotropic mixing instead of pulse-interrupted free precession for transfer of magnetization. Use of homonuclear isotropic mixing instead of COSY-type magnetization transfer can also yield increased sensitivity in numerous other J correlation experiments where magnetization is transferred between

nuclei with line widths larger than their mutual J coupling.

The cross-peak to diagonal-peak intensity ratios in the (HN)CO(CO)NH spectrum permit accurate measurement of $^3J_{C'C'}$. In this respect, it is interesting to note that the type of isotropic mixing scheme used affects the cross-peak to diagonal-peak ratio. For example, if the isotropic mixing scheme is applied with the rf field along the $\pm y$ -axis, orthogonal to that of the SL_x trim pulse, this results in an increase of the diagonal resonance intensity owing to favorable relaxation during the mixing scheme. In contrast, to a good approximation, the cross-peak intensity is not affected by the phase of the rf field during isotropic mixing in the limit of small J couplings. Thus, Eq. 8 only applies to continuous mixing schemes with the rf field aligned along the $\pm x$ -axis.

Acknowledgements

We thank Jin-Shan Hu for useful discussions. This work was supported by the AIDS Targeted Anti-Viral Program of the Office of the Director of the National Institutes of Health.

References

- Abragam, A. (1961) *The Principles of Nuclear Magnetic Resonance*, Oxford University Press, Oxford, U.K., p.70.
- Bax, A. and Davis, D.G. (1985) *J. Magn. Reson.*, **65**, 355–360.
- Braunschweiler, L. and Ernst, R.R. (1983) *J. Magn. Reson.*, **53**, 521–528.
- Ernst, R.R., Bodenhausen, G. and Wokaun, A. (1987) *Principles of Nuclear Magnetic Resonance in One and Two Dimensions*, Clarendon Press, Oxford, U.K., p. 445.
- Garrett, D.S., Kuszewski, J., Hancock, T.J., Lodi, P.J., Vuister, G.W., Gronenborn, A.M. and Clore, G.M. (1994) *J. Magn. Reson.*, **B104**, 99–103.
- Griesinger, C., Gemperle, C., Sørensen, O.W. and Ernst, R.R. (1987) *Mol. Phys.*, **62**, 295–308.
- Grzesiek, S. and Bax, A. (1993) *J. Am. Chem. Soc.*, **115**, 12593–12594.
- Grzesiek, S., Bax, A., Clore, G.M., Gronenborn, A.M., Hu, J.-S., Kaufman, J., Palmer, I., Stahl, S.J. and Wingfield, P.T. (1996) *Nat. Struct. Biol.*, **3**, 340–345.
- Hu, J.-S. and Bax, A. (1996) *J. Am. Chem. Soc.*, **118**, 8170–8171.
- Kay, L.E., Xu, G.Y. and Yamazaki, T. (1994) *J. Magn. Reson.*, **A109**, 129–133.
- Laskowski, R., Rullmann, J.A.C., MacArthur, M.W., Kaptein, R. and Thornton, J.M. (1996) *J. Biomol. NMR*, **8**, 477–486.
- Pardi, A., Billeter, M. and Wüthrich, K. (1984) *J. Mol. Biol.*, **180**, 741–751.
- Schleucher, J., Quant, J., Glaser, S.J. and Griesinger, S. (1995) In *Encyclopedia of Nuclear Magnetic Resonance*, Vol. 6 (Grant, D.M. and Harris, R.K., Editors-in-Chief), Wiley, London, U.K., pp. 4789–4804.
- Shaka, A.J., Lee, C.J. and Pines, A. (1988) *J. Magn. Reson.*, **77**, 274–293.
- Wang, A.C. and Bax, A. (1996) *J. Am. Chem. Soc.*, **118**, 2483–2494.
- Wüthrich, K. (1986) *NMR of Proteins and Nucleic Acids*, Wiley, New York, NY, U.S.A.